

DEPENDENCE OF SiAlON-TiN COMPOSITE PROPERTIES ON TiN REINFORCEMENT PARTICLE SIZE

Gökhan AÇIKBAŞ¹, Nurcan ÇALIŞ AÇIKBAŞ^{2,*}

¹Metallurgy Program, Vocational School, Bilecik Şeyh Edebali University, Bilecik, Turkey

²Metallurgical and Materials Engineering Department, Engineering Faculty, Bilecik Şeyh Edebali University, Bilecik, Turkey

ABSTRACT

In this study, the effect of TiN particle size (nano and micrometer level), being an effective parameter on microstructural evolution, mechanical and physical properties of SiAlON-TiN composites, was investigated. SEM and the XRD characterization methods were used to observe the effects of TiN particle size on the phase and microstructural evolution. Indentation fracture toughness and Vickers hardness of the manufactured specimens were measured in order to evaluate the mechanical behavior. Archimedes principle was used to determine the bulk density and porosity. Correlation between TiN particle size and hardness, fracture toughness, microstructure, phase evolution was discussed. It was observed that decrease in particle size led to little improvement in fracture toughness and hardness.

Keywords: SiAlON-TiN composites, TiN particle size, Microstructure, Hardness, Fracture toughness

1. INTRODUCTION

SiAlON ceramics are the most common materials which are used in diverse applications such as cutting tools, thermocouple protection tubes, non-ferrous molten metal handling, crucibles, wear parts, biomaterial, etc. due to high mechanical, corrosion, oxidation, wear, thermal shock resistance and high temperature properties [1-6]. However their performance sometimes is insufficient in several applications. In order to enhance properties of SiAlON ceramics, composite approach is applied [7]. SiC, TiN, TiC, TiCN, TiB₂, WC, MoSi₂ etc. phases are used as reinforcement for SiAlON matrix [8-17].

TiN has attracted much attention since it has high melting temperature (2940°C), extreme hardness, elastic modulus and electrical conductivity [18]. TiN incorporation into SiAlON matrix improves the strength, fracture toughness, thermal shock resistance and chemical wear resistance [19-25]. SiAlON-TiN composites are produced with different processing routes and sintering techniques such as gas pressure sintering, hot pressing, hot isostatic pressing and spark plasma sintering to obtain fully dense structures [19, 26-29]. They are good candidates for the production of complex shaped products with electrical discharge machining (EDM) due to high electrical conductivity [30, 31]. On the other side, TiN particles don't have any health risk in comparison with SiC whisker and it is possible to produce SiAlON-TiN composites with gas pressure sintering route which is suitable for serial production [3, 14, 15, 16]. In our previous studies, coarse TiN particles (d₅₀: ~2.9 µm) were incorporated in SiAlON matrix, and the influence of TiN addition on microstructural evolution, z value, densification, phase assemblage, thermal shock and wear resistance, was investigated [3, 32-34].

Reinforcement particle size affects the properties of ceramic-matrix composites [35, 36]. The mechanical properties of ceramics can be enhanced markedly by dispersing nanometer-sized particles in the ceramic matrix. For example, in cutting tool applications, coarse TiN particles provide more surface roughness and lead to more wear losses [37]. Nagaoka and co-workers studied the effect of 10 wt.% TiN with average particle sizes of 0.3, 1, 1.8, 3.7, 7.3, 13.6 µm, on elastic modulus, fracture

*Corresponding Author: nurcan.acikbas@bilecik.edu.tr

Receiving Date: 19 January 2018 Publishing Date: 29 June 2018

toughness and microstructure [38]. The results showed that the highest fracture toughness was obtained with TiN particles of size 4 μm and with the increase in particle size elastic modulus decreased. In literature there are very limited studies about the influence of TiN particle size on the properties of SiAlON ceramics [38]. Therefore, in this study, α/β SiAlON-TiN composites were fabricated with nano sized (40 nm) and sub-micron (0.5 μm) TiN powders. The effect of TiN particle size on mechanical and physical properties was investigated. The results were compared with the coarse particle size TiN containing SiAlON-TiN composites.

2. MATERIALS AND METHODS

2.1. Initial Powder Processing, Characterization, and Preparation of Composites

25 α' :75 β' -SiAlON composition was designed with z value of 0.7 by incorporation of 17 wt% TiN. The value of TiN content was decided by considering the results of our previous studies [32,33]. Two different TiN powders were used. The first one was obtained by milling coarse TiN powder (>99% pure, H.C. Starck, Grade C, Berlin, Germany) and the resulting average particle size was 2.9 μm (see Figure 1a). SEM analysis of as-received TiN powder was given in Figure 2a. As-received TiN powder exhibited irregular morphology with sharp edge and about 3 μm in size. The coarse TiN powder (d_{50} : 2.91 μm) was milled in deionised water in planetary mill with % 67 solid loading for 10 hours at 350 rpm to reduce particle size to 0.5 μm by using Si_3N_4 balls with 3 mm diameter. Milling efficiency was given in Fig 3. SEM analysis of milled TiN powder was given in Figure 2b. SEM analysis showed that the powders after milling showed a wide particle sizes distribution. Some of the particles were of very fine particle size of approximately 0.3 μm and some others were coarse particles with sizes around 1.5 μm . Laser diffraction method also supported the SEM images (Figure 4). The laser diffraction particle size distribution graph indicated a mean particle size of 0.42 μm in the range of 0.1–1.99 μm with two peaks for highest volume percent of 0.2 and 1.5 μm particle sizes.

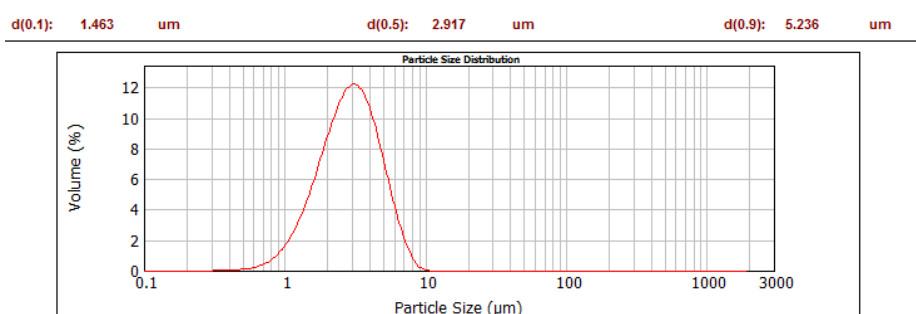


Figure 1. Particle size distribution graph of as-received TiN powder (H.C. Starck, Grade C)

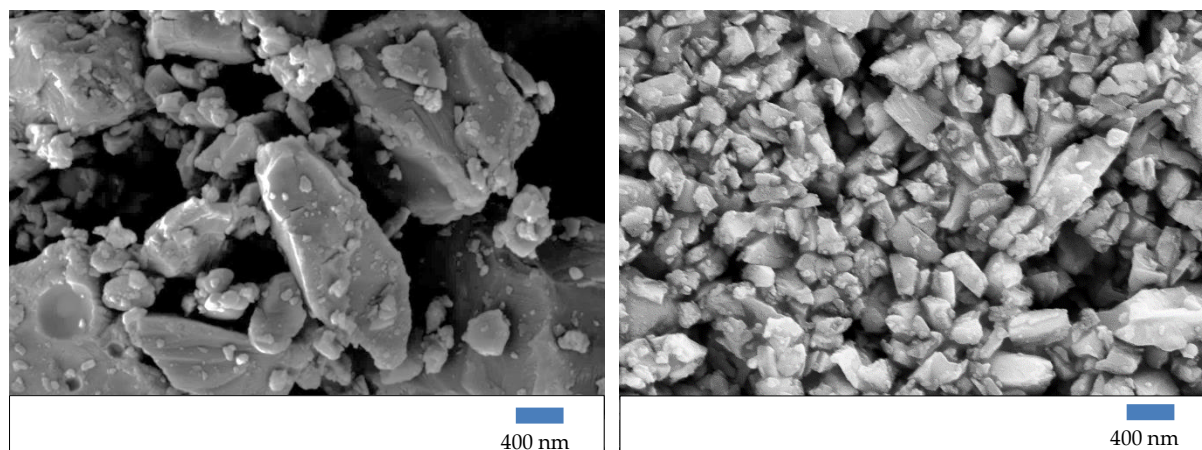


Figure 2. SEM-SE image of (a) as-received TiN powder, (b) after 10 hours milling

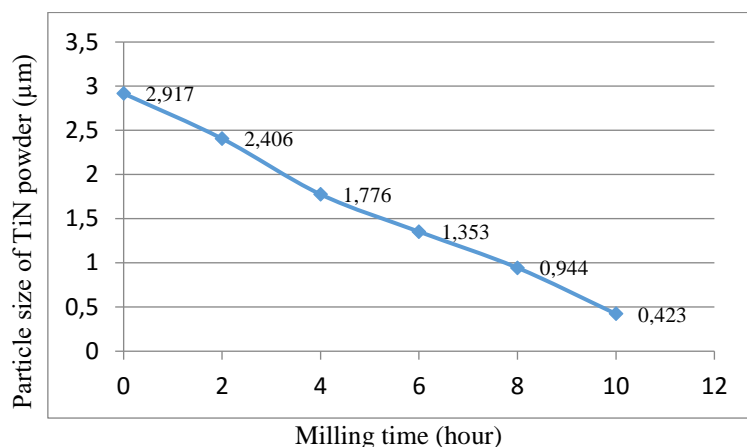


Figure 3. Particle size reduction with milling time

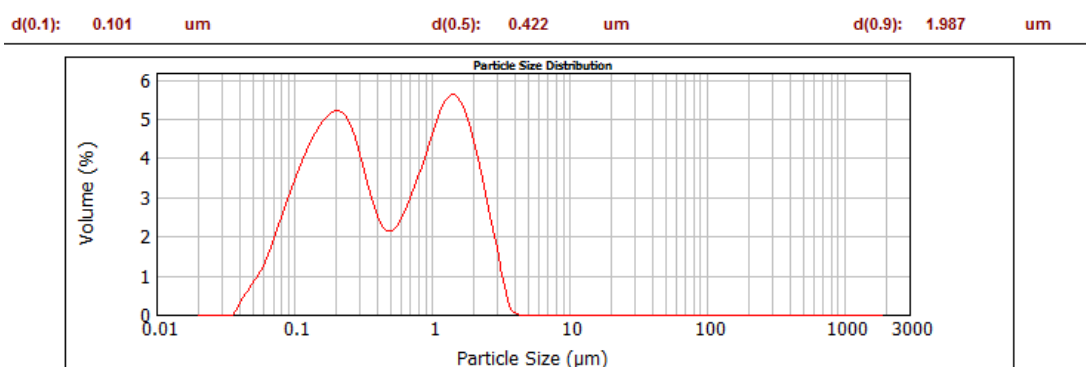


Figure 4. Particle size distribution graph of milled TiN powder

Nano TiN powder of average particle size of 45 nm (surface area $30 \pm 2 \text{ m}^2/\text{gr}$, $21.2 \pm 0.2 \text{ wt.\%N}$, 0.3 wt.\%O and 0.05 wt.\%C , Plasma Ceramic Technologies Ltd., Salaspils, Latvia) was used. Due to finer and non-spherical particle shape of the nano powder, particle size distribution could not be measured by laser diffraction method. SEM-SE analysis of nano TiN powder was given in Figure 5. The nano TiN powders were in cubic and triangular prism shape and the particle size was in between 10-70 nm.

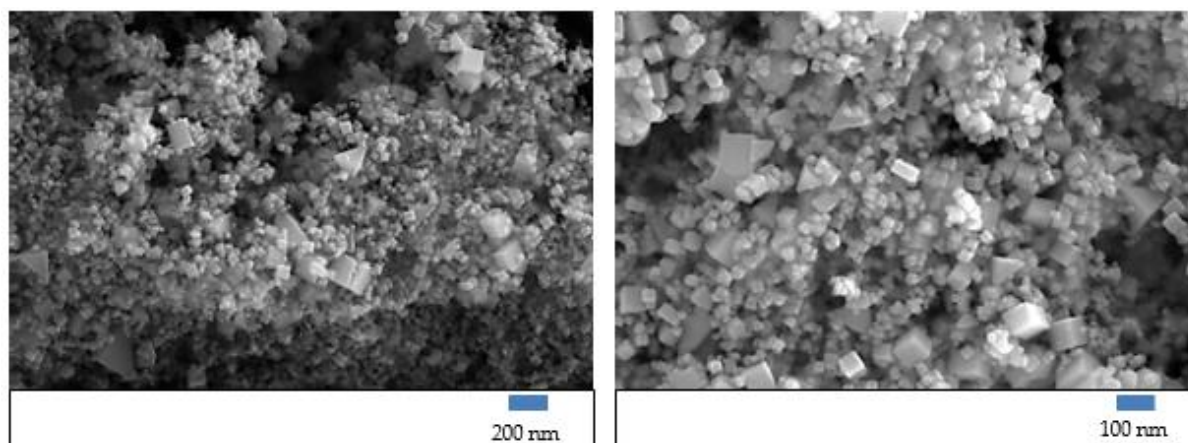


Figure 5. SEM-SE image of as-received nano TiN powder in different magnifications (a) 100.000x, (b) 200.000x

α' : β' -SiAlON composites with 25 α' :75 β' phase ratio and 0.7 z value were prepared with the addition of 17 wt.% nano and submicron sized TiN powders. High purity α -Si₃N₄ powder (E-10 grade, UBE Co.

Ltd., Japan) and AlN powder (H Type, Tokuyama Corp. Japan), Al₂O₃ (Alcoa A16-SG, Pittsburgh, USA), Yb₂O₃ (>99.99%, Treibacher, Austria), Sm₂O₃ (>99.9%, Stanford Materials Corp., USA), CaCO₃ (>99.75%, Reidel-de Haen, Germany) powders were used for compositional design.

SiAlON-TiN composite production procedures were given in the following chart (Figure 6). Nano sized powder was dispersed in pure water with dispersant (TMAOH) and then exposed to ultrasonic treatment for 30 minutes to prevent powder agglomeration. The designed compositions were prepared by planetary milling for 90 min at 300 rpm in isopropyl alcohol using Si₃N₄ balls. Since the milling conditions of nitride based powders are known to affect the subsequent microstructure and mechanical properties, these milling conditions were specifically chosen [39]. Colloidal TiN solution was introduced into the SiAlON slurry and then mixing was carried out in mixer. Rotary evaporator was used for drying slurries and then the powders were dry sieved with a mesh size of 150 µm.

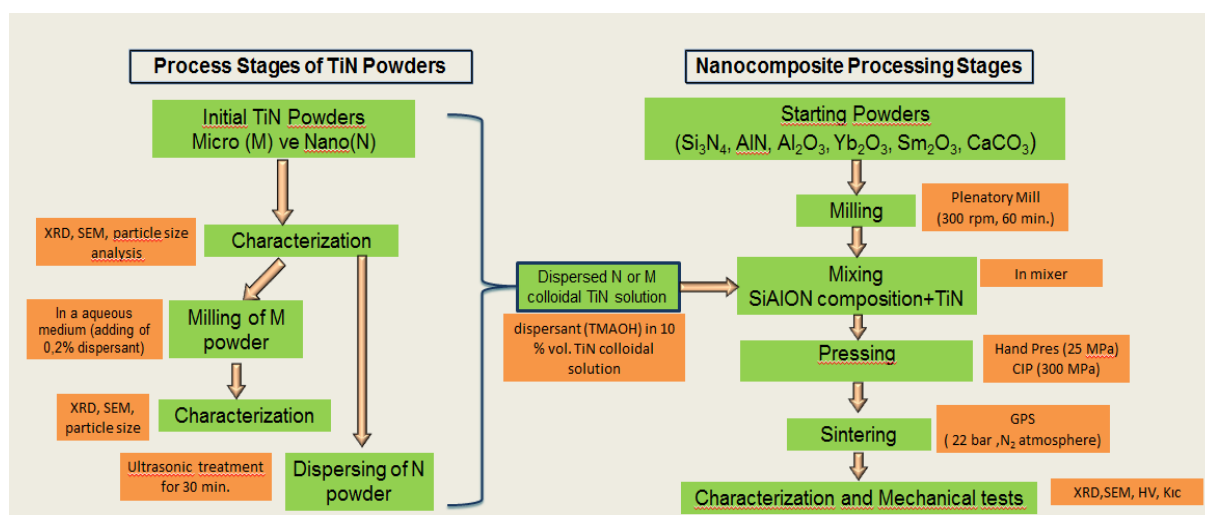


Figure 6. SiAlON-TiN composite production process flow chart

The SiAlON-TiN compositions were uniaxially pressed to a maximum pressure of 25 MPa and subsequently cold isostatically pressed at 300 MPa to increase the green density. The pellets were sintered using a two-step gas pressure sintering cycle with a maximum of 2.2 MPa nitrogen gas pressure at 1890°C for 90 min and then the furnace was allowed to cool at a rate of 5°C/min.

2.2. Characterization of Composites

Sintered sample's density and open porosity % values were obtained by Archimedes principle. X-ray diffraction analyses (XRD-Panalytical, Empeyrean with Cu-K α radiation) was used to determine α' : β' -SiAlON phase ratios and intergranular phase composition. The α' : β' -SiAlON phase ratios were found by quantitative estimation from the XRD patterns using the integrated intensities of the (102) and (210) reflections of α' -SiAlON and the (101) and (210) reflections of β' -SiAlON by the following equation:

$$\frac{I_{\beta}}{I_{\beta} + I_{\alpha}} = \frac{1}{1 + K \left[\left(\frac{1}{w_{\beta}} \right) - 1 \right]} \quad (1)$$

where I_{α} and I_{β} are observed intensities of α' and β' -SiAlON peaks, respectively, w_{β} is the relative weight fraction of β' -SiAlON, and K is the combined proportionality constant resulting from the constants in the two equations, namely:

$$I_{\beta} = K_{\beta} * W_{\beta} \quad (2)$$

$$I_{\alpha} = K_{\alpha} * W_{\alpha} \quad (3)$$

which is (0.518 for β (101) – α (102) reflections and 0.544 for β (210) – α (210) reflections [40].

The cell parameters of β^1 -SiAlON were measured with silicon powders as the internal standard. The z-value of the β^1 -SiAlON phase was obtained from the mean of z_a and z_c values given by the following equations:

$$z_a = \frac{a - 7.6044}{0.031} \quad (4)$$

$$z_c = \frac{c - 2.9075}{0.026} \quad (5)$$

Microstructural investigations were carried out by Zeiss Supra 40VP FEG-SEM. Vickers indentation technique was used for hardness measurement and indentation fracture (IF) toughness was calculated. Vickers hardness tests were carried out under 98 N load. The Vickers hardness (HV) was calculated by the following equation (Evans and Charles): [41]

$$HV10 = 0.47P/a^2 \quad (6)$$

where, HV10 is the Vickers hardness, P is load applied and a is half the length of the diagonal of the indentation produced by the indenter. Indentation fracture toughness (K_{IC}) was calculated by the hardness tests using the formula proposed by Niihara et al for median cracks:[42]

$$K_{IC} = 0,018 * HV * a^{0.5} * (E/HV)^{0.4} * (c/a - 1)^{-0.5} \quad (\text{for } c/a < 3.5 \text{ and } l/a < 2.5) \quad (7)$$

where 2a is the average indent diagonal length (μm), 2c is the crack length (from one crack tip to another), E is the elastic modulus (GPa) which is taken as a constant equivalent to 320 GPa for all the samples and H is the measured hardness (GPa). The crack length and indent diagonal were measured from optical images of the indented surfaces. 3 samples tested for each composition with 5 indents and the standard deviation was calculated.

3. RESULTS AND DISCUSSION

The physical, mechanical, microstructural and phase characterization were carried out on developed nano and micron size TiN incorporated SiAlON composites. Table 1 shows the some properties of developed composites. Micron size TiN powder containing composite was coded as S-TM and nano size TiN containing composite coded as S-TN. The SiAlON compositions were designed to obtain 75 β^1 :25 α^1 phase ratios and 0.7 of z value. The results showed that aimed phase ratios and z value were achieved. The XRD patterns of developed composites were given in Figure 7. According to XRD pattern intergranular phase was amorphous but little amount of oxygen rich Yb₃Al₅O₁₂ (YbAG) phase existed. In our previous study, we observed that intergranular phase chemistry was affected by z value and Jss phase was predominantly stable when the z value was low (0.3-0.4) [32]. With the increment in z value over 0.74 crystallization tendency of the intergranular phase was weaker. With further increase in z value (>0.80) the stable phase was YbAG. However, in this case the z value of SiAlONs is ~0.65 and amorphous phase is predominant with a little amount of stable YbAG phase. This can be related to the oxygen content of the system/composition. The source of the differences is IGP are TiN particle sizes in the compositions. In the former composition coarse TiN powder with average particle size was ~2.9 micron while in this study nano TiN powder (40 nm) and milled TiN powder (0.5 micron) was used. TiN powder surface may be coated with its oxide of TiO₂ with thin layer after milling and hence the compositions will be rich in oxygen. This phenomenon may lead to formation of

oxygen rich YbAG phase instead of Jss. The EDX analysis of TiN powders confirmed the formation of TiO₂ layer (Figure 8, 9). Therefore instead of Jss phase, amorphous and a little amount of YbAG phase were available as grain boundary phases.

Table 1. Properties of the developed SiAlON-TiN composites

	S-TM	S-TN
$\beta^1:\alpha^1$ SiAlON phase ratios	76 β : 24 α	77 β : 23 α
z value	0.65	0.64
IGP	Amorphous and Yb ₃ Al ₅ O ₁₂	Amorphous and Yb ₃ Al ₅ O ₁₂
HV10 (GPa)	16.76±0.29	16.81±0.18
K _{1c} (MPam ^{1/2})	6.75±0.21	7.12 ± 0.42
Density (g/cm ³)	3.4994	3.4873
Open Porosity %	0.14	0.05

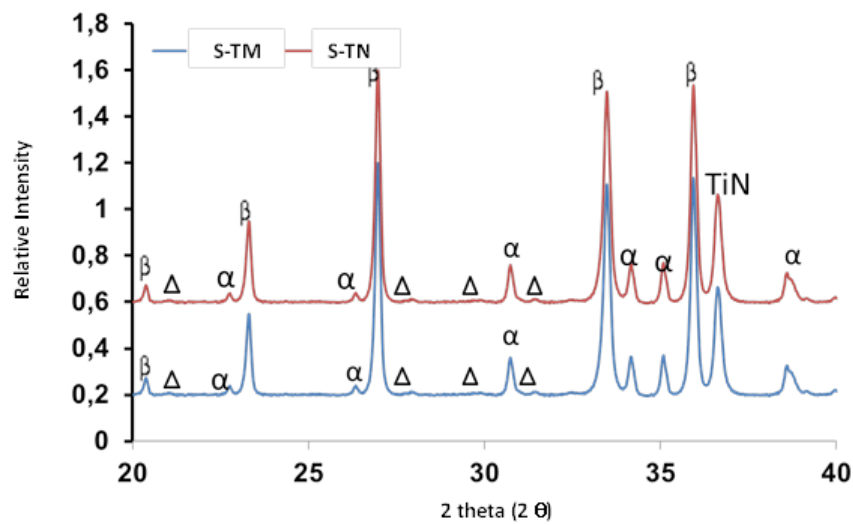


Figure 7. XRD spectra of SiAlON-TiN composites (Δ :Yb₃Al₅O₁₂, β : β^1 -SiAlON, α : α^1 -SiAlON)

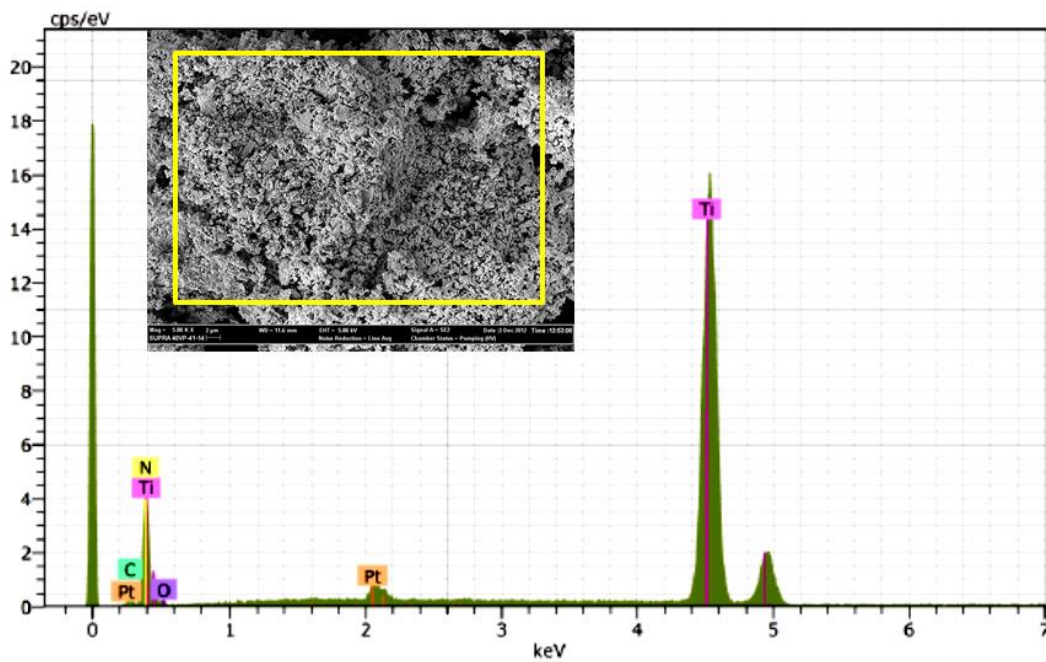


Figure 8. SEM-EDX analysis of milled TiN powder

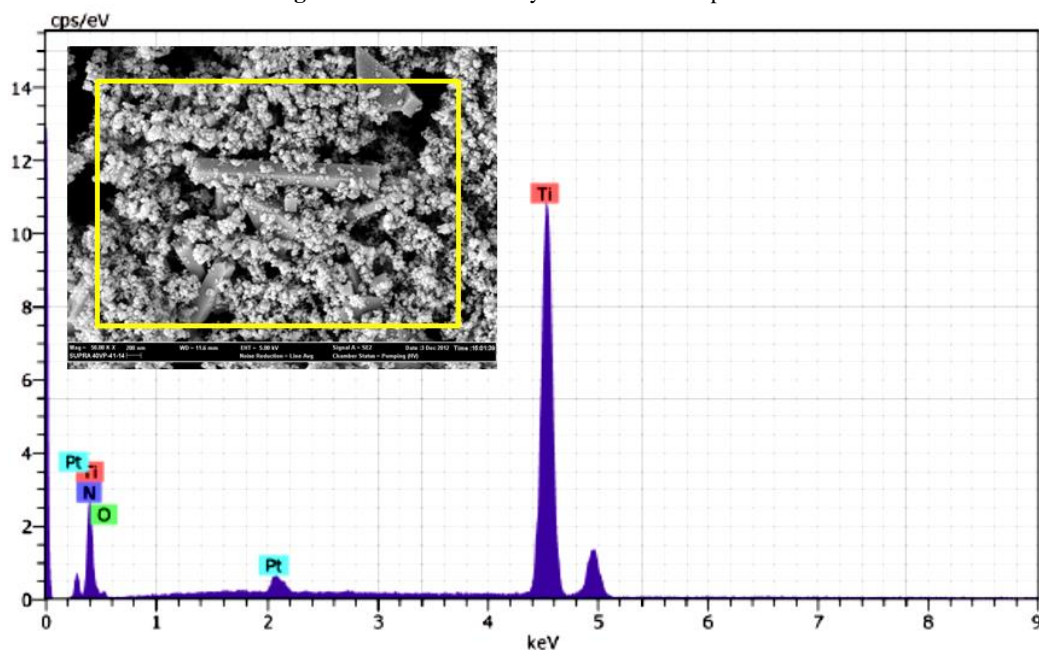


Figure 9. SEM-EDX analysis of nano TiN powder

According to density measurements by Archimedes Principle the samples had 3.4994 and 3.4873 g/cm^3 bulk densities for S-TM and S-TN, respectively. Open porosity content of samples 0.14 for S-TM and 0.05% for S-TN samples. Microstructural images of both compositions are given in Figure 11, 12. The microstructure of the samples revealed the presence of three different contrasting phases. The elongated grains with dark gray colored were β '-SiAlON, the equiaxed grains with light grey were α '-SiAlON, the grains with sharp contrast were TiN due to the strong electron-scattering of the Ti atoms. Agglomerations of nano particles were available in some regions of S-TN and S-TM sample microstructures. S-TM samples with coarser TiN particle sizes (500 nm) had less tendency of agglomeration than S-TN samples. This indicated that ultrasonic treatment was not sufficient to disperse nano sized powders. Therefore nano TiN particle clusters were observed in microstructure.

According to mechanical tests, standard deviation was in between ± 0.18 and 0.29 for hardness and 0.21 and 0.42 for fracture toughness. The standard deviation was higher for S-TN composition due to inhomogeneity in microstructure (see Figure 10). On the other hand S-TM composition showed more homogeneous distribution of TiN particles in the microstructure and standard deviation was lower (Figure 11). With the decrease of tenfold in the particle size (500 nm to 40 nm) homogeneous mixing of powders was getting harder. Crack profile of samples analyzed by SEM in order to study the crack propagation behavior. Several fracture toughness mechanisms were effective for silicon nitride based ceramics, namely, microcracking, crack bridging and crack deflection [33,43]. As can be seen from Figure 12a, b crack deflection and bridging were the main toughening mechanisms. Owing to high aspect ratio grains ($7 <$) fracture toughness of both compositions was high (6.75 and 7.12 $\text{MPam}^{1/2}$). Besides, because of the difference between the thermal expansion coefficient values of TiN and SiAlON grains, microcracking around the TiN particles were observable. This mechanism could be effective for toughening of composite [24, 38]. In this case, the fracture toughness increased with the decreasing particle size. However, the changes in fracture toughness were not significant ($\sim 5.5\%$). Since the fracture toughness of SiAlON based materials could be controlled mainly by microstructure, changes in microstructure influenced the fracture toughness [33, 39]. For example aspect ratio of grains, grain size, bonding between the grain and grain boundary, z value affected the fracture toughness. Since both samples had similar aspect ratio grains (3-7), the fracture toughness values were

close. On the other hand, both compositions had similar intergranular phase chemistry and probably had similar bonding strength between the grain and grain boundary phases.

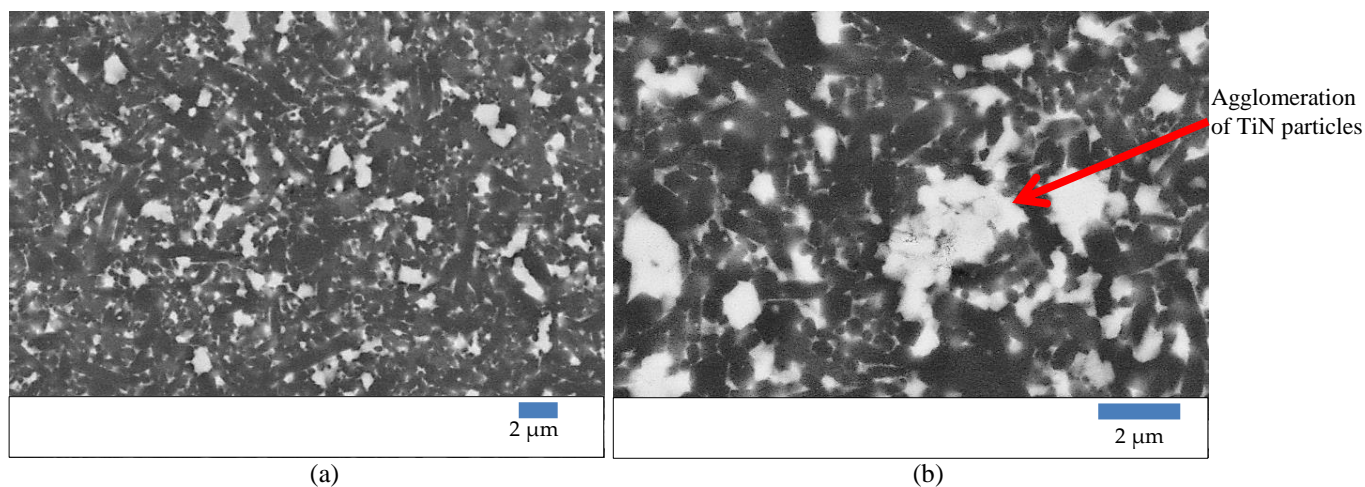


Figure 10. Representative BSE image of S-TN samples in different magnifications (a) 10.000x, (b) 20.000x (arrow shows the agglomeration of nano TiN particles)

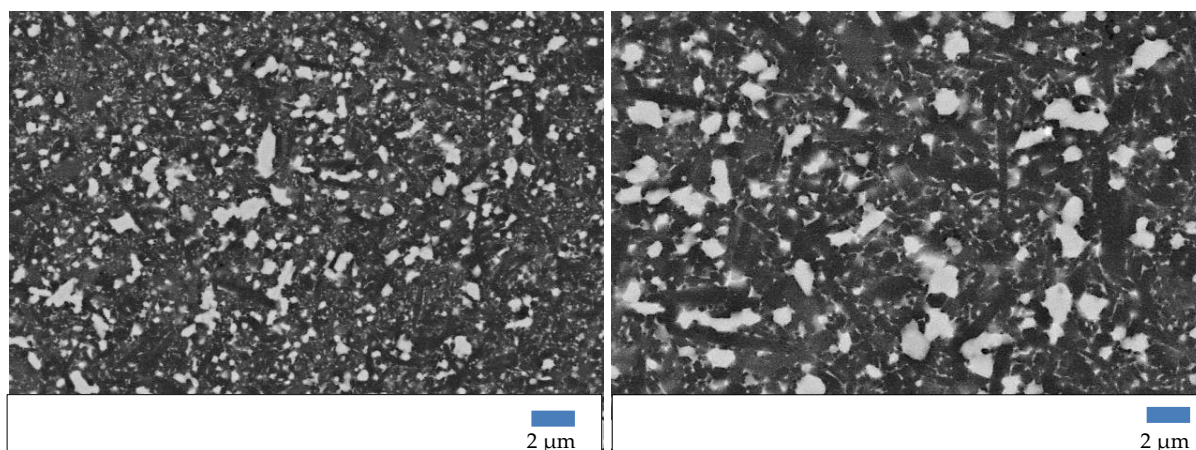


Figure 11. Representative BSE image of S-TM samples in different magnifications (a) 5.000x, (b) 10.000x

The hardness value was kept as almost similar since the hardness of SiAlON ceramics was controlled mainly by phase content (α' : β' -SiAlON phase ratios and the content of IGP) and porosity. The α' to β' -SiAlON phase ratios and porosity content were almost the same in both compositions. The other affecting parameters on hardness were grain size, shape and orientations, intergranular phase nature/composition, second phase(s), z value etc. In our previous study while the SiAlON-TiN composites had different z values (0.43-0.91), similar hardness values were obtained due to similar α' : β' -SiAlON phase ratios and porosity content [32]. In our previous study, the hardness value was 16.48 GPa and fracture toughness was 7 MPam^{1/2} for 81 β' :19 α' -SiAlON phase ratio and 17 wt.%TiN content (d_{50} :2.9 micron) composite [33]. When comparing the hardness and fracture toughness values of composites containing TiN particle sizes of 40 nm and 0.5 micron with TiN particle sizes of 2 microns, no enhancement on mechanical properties was observed. This could be a result of the agglomeration of fine TiN particles in SiAlON matrix. If TiN particles were well dispersed in SiAlON matrix, the hardness and fracture toughness could be enhanced with a decrease in TiN particle size.

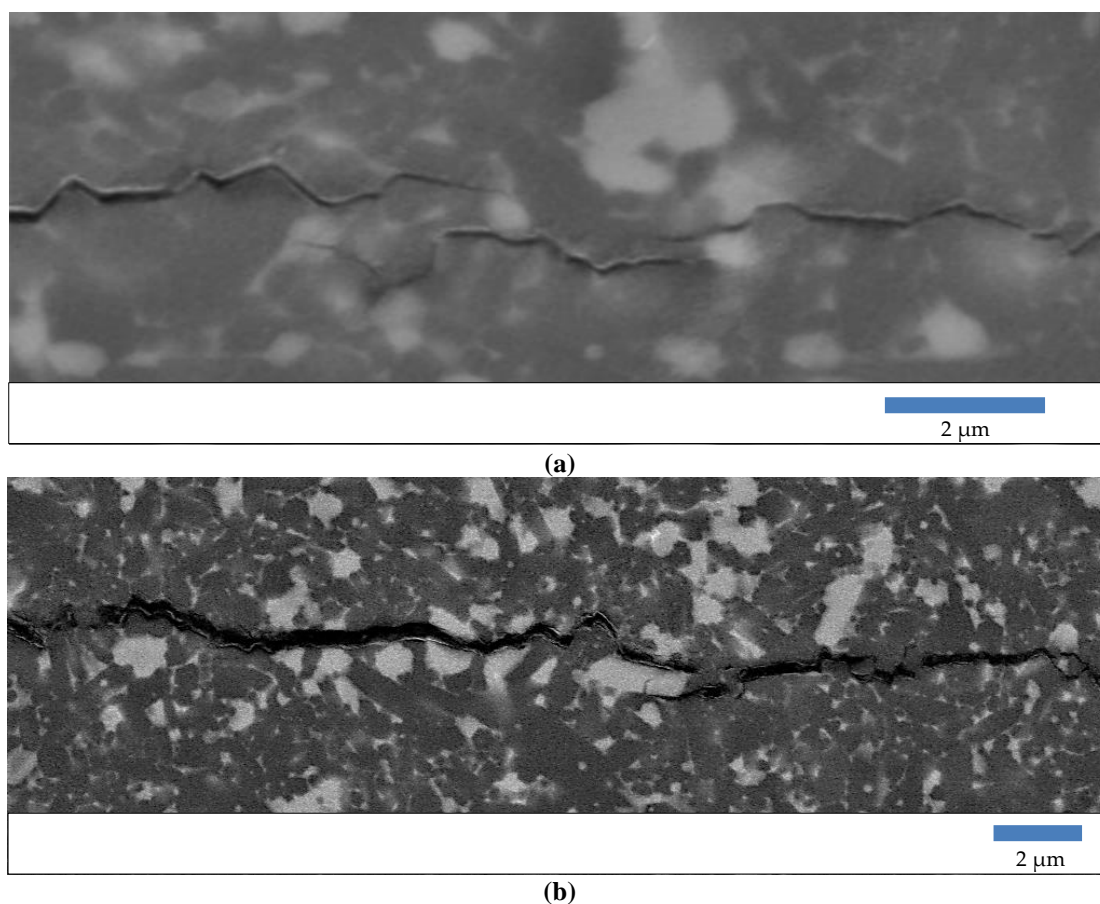


Figure 12. Crack profile of SiAlON-TiN composites (a) S-TM, (b) S-TN

4. CONCLUSIONS

In this study, how the changes in TiN particle sizes (40 nm and 500 nm) governed the microstructural, physical and mechanical properties were investigated. Obtained results were compared with previous studies where the average TiN particle size was about 3 microns. The microstructural investigations showed that nano TiN powder could not be well dispersed in SiAlON matrix. Therefore TiN particle clusters were observed in the microstructure. Expected improved mechanical properties in terms of hardness and fracture toughness were not achieved due to particle clusters. It was observed that decrease in TiN particle size from 2.9 microns to 40 nm and 500 nm did not have any positive effect on hardness and fracture toughness. On the other hand, intergranular phase chemistry was changed by decreasing TiN particle size from micron to nano size scale. With the more homogeneous distribution of fine TiN grains in SiAlON matrix an enhancement in mechanical properties can be achieved.

REFERENCES

- [1] Li W, Zhang B, Zhuang H, Li W. Effect of TiN on the corrosion behavior of Y-(α + β)-SiAlON/TiN materials in hot hydrochloric acidic solutions. *Ceram Int* 2005; 31(2):277-280.
- [2] Jiang T, Xue XX, Li Zf, Duan PN. High temperature oxidation behavior of electroconductive TiN/O'-SiAlON ceramics prepared from high titania slag-based mixture. *T Nonferr Metal Soc* 2011;21(12):2638-43.

- [3] Acikbas NC, Tegmen S, Ozcan S, Acikbas G. Thermal shock behaviour of α : β -SiAlON–TiN composites. *Ceram Int* 2014; 40(2):3611-8.
- [4] Kumar A, Mallik AK, Acikbas NC, Yaygingol M, Kara F, Mandal H, Basu D, Biswas K, Basu B. Cytocompatibility property evaluation of gas pressure sintered SiAlON–SiC composites with L929 fibroblast cells and Saos-2 osteoblast-like cells. *Materials Science and Engineering: C*. 2012; 32(3):464-9.
- [5] Kumar R, Acikbas NC, Kara F, Mandal H, Basu B. Microstructure–mechanical properties–wear resistance relationship of SiAlON ceramics. *Metall Mater Trans A*. 2009; 40(10):2319-32.
- [6] Riley F. Silicon nitride and related materials. *J Am Ceram Soc* 2000; 83: 245-265.
- [7] Hong F, Lewis MH. Ceramic-Matrix Composites Via in-Situ Reaction Sintering. In *Proceedings of the 17th Annual Conference on Composites and Advanced Ceramic Materials, Part 2 of 2: Ceramic Engineering and Science Proceedings, Volume 14, Issue 9/10 2009 Sep 28* (pp. 699-706). John Wiley & Sons, Inc.
- [8] Akin SR, Turan S, Gencoglu P, Mandal H. Effect of SiC addition on the thermal diffusivity of SiAlON ceramics. *Ceram Int* 2017; 43(16):13469-74.
- [9] Vleugels J, Jiang DT, Van der Biest O. Development and characterisation of SiAlON composites with TiB₂, TiN, TiC and TiCN. *J Mater Sci* 2004; 39(10):3375-81.
- [10] Bitterlich B, Bitsch S, Friederich K. SiAlON based ceramic cutting tools. *J Eur Ceram Soc* 2008; 28(5):989-94.
- [11] Ayas E, Kara A, Kara F. α/β SiAlON based composites incorporated with MoSi₂ for electrical applications. In: Singh D, Zhu D, Zhou Y, editors. *Design, Development and Applications of Engineering Ceramics and Composites*. USA: Ceramic Transactions, 2010. pp. 189-195.
- [12] Kumar Mallik A, Madhav Reddy K, Calis Acikbas N, Kara F, Mandal H, Basu D, Basu B. Influence of SiC addition on tribological properties of SiAlON. *Ceram Int* 2011; 37: 2495–2504.
- [13] Ayas E, Kara A. Novel electrically conductive α/β SiAlON/TiCN composites. *J Euro Ceram Soc* 2011; 31: 903–911.
- [14] Ayas E. Mechanical, electrical and thermal properties of α/β SiAlON-SiC composites fabricated by gas pressure sintering method. *Anadolu University of Sciences & Technology-A: Applied Sciences & Engineering*. 2016;17(5).
- [15] Ayas E, Kara A, Mandal H, Turan S, Kara F. Production of alpha-beta SiAlON-TiN/TiCN composites by gas pressure sintering. *Silic Ind* 2004; 69(7):287-92.
- [16] Nordberg LO, Ekström T. Hot-Pressed MoSi₂-Particulate-Reinforced α -SiAlON Composites. *J Am Ceram Soc* 1995; 78(3):797-800.
- [17] Mallik AK, Acikbas NC, Kara F, Mandal H, Basu D. A comparative study of SiAlON ceramics. *Ceram Int*. 2012; 38(7):5757-67.
- [18] Graziani TB, Bellosi AB. Densification and characteristics of TiN ceramics. *J Mater Sci* 1995; 14(15):1078-81.

- [19] Smirnov KL. β -SiAlON-TiN/TiB₂. *Int J Self-Propag High-Temp Synth* 2016; 25(2):80-5.
- [20] Desmaison J, Desmaison M. Boride/nitride composites: synthesis and properties. In *Materials Science of Carbides, Nitrides and Borides 1999* (pp. 267-284). Springer Netherlands.
- [21] Blugan G, Hadad M, Janczak-Rusch J, Kuebler J, Graule T. Fractography, mechanical properties, and microstructure of commercial silicon nitride–titanium nitride composites. *J Am Ceram Soc* 2005; 88(4):926-33.
- [22] Ayas E, Kara A, Kara F. A novel approach for preparing electrically conductive α/β SiAlON-TiN composites by spark plasma sintering. *J Ceram Soc Jap* 2008; 116(1355):812-4.
- [23] Duan RG, Roebben G, Vleugels J, Van der Biest O. Optimization of microstructure and properties of in situ formed β -O-SiAlON–TiN composite. *Mater Sci Eng: A*. 2006; 427(1):195-202.
- [24] Xu F, Wen S, Nordberg LO, Ekström T. TEM study of Y-doped α -SiAlON composite with 10 vol% TiN particulates. *Mater Lett* 1998; 34(3):248-52.
- [25] Ekström T, Olsson PO. β -SiAlON ceramics with TiN particle inclusions. *J Euro Ceram Soc* 1994; 13(6):551-9.
- [26] Hong F, Lumby RJ, Lewis MH. TiN/SiAlON composites via in-situ reaction sintering. *J Euro Ceram Soc* 1993; 11(3):237-9.
- [27] Krnel K, Maglica A, Kosmač T. β -SiAlON/TiN nanocomposites prepared from TiO₂-coated Si₃N₄ powder. *J Euro Ceram Soc* 2008; 28(5):953-7.
- [28] Shimada S, Kato K. Coating and spark plasma sintering of nano-sized TiN on Y- α -SiAlON. *Mater Sci Eng: A*. 2007; 443(1):47-53.
- [29] Lenčič Z, Šajgalík P, Toriyama M, Brito ME, Kanzaki S. Multifunctional Si₃N₄/(β -SiAlON+TiN) layered composites. *J Euro Ceram Soc* 2000; 20(3):347-55.
- [30] Bellosi A, Guicciardi S, Tampieri A. Development and characterization of electroconductive Si₃N₄-TiN composites. *J Euro Ceram Soc* 1992; 9(2):83-93.
- [31] Trueman CS, Huddleston J. Material removal by spalling during EDM of ceramics. *J Euro Ceram Soc* 2000; 20(10):1629-35.
- [32] Acikbas NC, Kara F. The effect of z value on intergranular phase crystallization of α / β 1-SiAlON-TiN composites. *J Euro Ceram Soc* 2017; 37(3):923-30.
- [33] Acikbas NC, Demir O. The effect of cation type, intergranular phase amount and cation mole ratios on z value and intergranular phase crystallization of SiAlON ceramics. *Ceram Int* 2013; 39(3):3249-59.
- [34] Acikbas NC. Tribological Behaviour of SiAlON-TiN Composites. *J Euro Ceram Soc*. DOI:10.1016/j.jeurceramsoc.2018.01.013
- [35] Niihara K, Nakahira A. Strengthening and toughening mechanisms in nanocomposite ceramics. In *Annales de chimie* 1991 (Vol. 16, No. 4-6, pp. 479-486). Lavoisier.

- [36] Niihara K. New design concept of structural ceramics. *J Ceram Soc Jap* 1991; 99(1154):974-82.
- [37] Acikbas NC, Ozcan S, Acikbas G. The effect of surface roughness on tribological behavior of SiAlON-TiN composites. II. INES International Academic Research Congress Abstract Book, 18-21 October 2017-Alanya/ANTALYA, pp. 584.
- [38] Nagaoka T, Yasuoka M, Hirao K, Kanzaki S. Effects of TiN particle size on mechanical properties of Si₃N₄/TiN particulate composites. *J Ceram Soc Jap* 1992; 100(1160):617-620.
- [39] Özcan S, Açıkbaş G, Özbay N, Açıkbaş NÇ. The effect of silicon nitride powder characteristics on SiAlON microstructures, densification and phase assemblage. *Ceram Int* 2017; 43(13):10057-65.
- [40] Liddell K. X-ray Analysis of Nitrogen Ceramic Phases MSc. Thesis, University of Newcastle, Upon Tyne, UK, 1979.
- [41] Evans AG, Charles EA. Fracture toughness determinations by indentation. *J Amer Ceram Soc* 1976; 59(7-8):371-372.
- [42] Niihara K, Morena R, Hasselman DP. Evaluation of K_{Ic} of brittle solids by the indentation method with low crack-to-indent ratios. *J Mater Sci Lett* 1982; 1(1):13-6.
- [43] Zhang C, Sun WY, Yan DS. Optimizing mechanical properties and thermal stability of Ln- α - β -sialon by using duplex Ln elements (Dy and Sm). *J Euro Ceram Soc* 1999; 19(1):33-9.